HHS Public Access

Author manuscript

J Comput Assist Tomogr. Author manuscript; available in PMC 2017 January 01.

Published in final edited form as:

J Comput Assist Tomogr. 2016 ; 40(1): 102–108. doi:10.1097/RCT.0000000000000312.

IMPROVED SEMI-AUTOMATED 4D-FLOW MRI ANALYSIS IN THE AORTA IN PATIENTS WITH CONGENITAL AORTIC VALVE ANOMALIES VS TRICUSPID AORTIC VALVES

Susanne Schnell, PhD, **Pegah Entezari, MD**, **Riti J. Mahadewia, BS**, **S. Chris Malaisrie, MD**, **Patrick M. McCarthy, MD**, **Jeremy D. Collins, MD**, **James Carr, MD**, and **Michael Markl, PhD**

Abstract

Objective—To systematically investigate a newly developed semi-automated workflow for the analysis of aortic 4D-flow MRI and its ability to detect hemodynamic differences in patients with congenitally altered aortic valve (CAV, bicuspid or quadricuspid valves) compared to tricuspid aortic valves (TAV).

Methods—4D-flow MRI data were acquired in 20 aortic dilation patients (9 TAV, 11 CAV). A semi-automated workflow was evaluated regarding inter-observer variability, accuracy of net flow, regurgitant fraction and peak systolic velocity, and the ability to detect differences between cohorts. Results were compared to manual segmentation of vessel contours.

Results—Despite the significantly reduced analysis time a good inter-observer agreement was found for net flow and peak systolic velocity and moderate agreement for regurgitation. Significant differences in peak velocities in the descending aorta (P=0.014) could be detected.

Conclusions—4D-flow MRI-based semi-automated analysis of aortic hemodynamics can be performed with good reproducibility and accuracy.

Keywords

4D Flow MRI; optimized workflow; aortic valve; aorta

INTRODUCTION

Time-resolved (CINE) 3D phase-contrast (PC) MRI[1,2] with velocity encoding along three spatial directions (also termed '4D-flow MRI')[3] has been widely used for the assessment of 3D blood flow in a number of clinical applications[4–16]. Visualization of complex 3D blood flow patterns and quantification of regional flow characteristics is possible with 4D-flow MRI[8,17–20].

Blood flow quantification using standard CINE 2D PC MRI based on single 2D analysis planes at a vascular region of interest has been extensively validated in the literature. Previous studies demonstrated that velocity assessment in the aorta and pulmonary artery is

Corresponding Author: Susanne Schnell, Northwestern University, Dept. of Radiology, 737 North Michigan Avenue, Suite 1600, Chicago, IL 60613, USA, Telephone: 1-312-695-3099, Fax: 1-312-926-5991, susanne.schnell@northwestern.edu.

reliable and comparable with Doppler ultrasound[13,21–23]. Other studies found high reproducibility for 2D PC MRI flow quantification in the pulmonary venous system and in a pulsatile flow phantom[24,25] as well as low intra- and interobserver variability for quantifying mitral flow[26].

In a recent healthy volunteer study investigating scan-rescan and inter- and intraobserver variability, it was shown that regional quantification of flow parameters based on aortic 4D-flow MRI in normal volunteers can also be performed with good reproducibility[27]. However, this study was based on time-consuming and labor intensive manual segmentation of the aortic lumen at user-defined anatomic regions of interest. A more automated analysis of 4D-flow MRI data would thus be desirable as it has the potential to reduce analysis time and may enable broader clinical applications. However, accuracy, reproducibility, and observer variability determine the potential utility of new methods for clinical applications[2,27].

Therefore, the scope of this study was to assess a new semi-automated workflow for blood flow visualization and calculation of quantitative parameters including peak velocity, net flow, and regurgitant fraction. We investigated inter-observer variability of the new semi-automated workflow, parameter accuracy compared to manual analysis as the reference standard, and differences in above mentioned metrics of hemodynamics in aortic dilation patients with congenitally altered aortic valves compared to tricuspid aortic valves.

MATERIALS AND METHODS

Study Population

Twenty patients (14 males, age = 50.7 ± 8.7 years) with aortic dilation were included in the study, divided into two groups. 11 patients (6 males, age = 46.7 ± 8.9 years) presented with a congenitally altered aortic valve (CAV cohort): 10 patients with bicuspid aortic valve (BAV) and one patient with a quadricuspid aortic valve. The second group consisted of 9 aortic dilation patients (8 males, age = 55.5 ± 5.9 years) with tricuspid aortic valves (TAV cohort). Aortic dilatation was defined at the sinuses of Valsalva (SOV) (SOV diameter$_{_CAV}$ = 4.2 ± 0.6 cm, SOV diameter$_{_TAV}$ = 4.3 ± 0.5 cm). The study was approved by the Institutional Review Board (IRB). All patients were included in accordance with an IRB protocol permitting retrospective chart review.

Data acquisition

All examinations were performed on a 1.5 T MR system (AVANTO, Siemens Germany). All subjects underwent a standard-of-care thoracic cardiovascular MRI including ECG gated time-resolved (CINE) cardiac MRI for the evaluation of cardiac function and valve morphology as well as contrast enhanced MR angiography for the quantification of aortic dimensions. For valve imaging, a 2D imaging plane was carefully positioned orthogonal to the aortic root at the level of the aortic valve. For the assessment of aortic hemodynamics, time-resolved 3D phase-contrast MRI with three-directional velocity encoding (4D-flow MRI) was employed to measure 3D blood flow velocities with full volumetric coverage of the thoracic aorta. Scan parameters were as follows: TE/TR = 2.27 – 2.41 ms / 1.42 – 3.13

ms, flip angle 15°, temporal resolution = 37.6–38.4 ms, bandwidth = 446–453 Hz/pixel, spatial resolution = 2.88 – 3.05×2.13 – 2.25×2.5 – 3.2 mm^3, parallel imaging (GRAPPA) along phase encoding direction (y) with reduction factor R = 2 (24 reference lines). The velocity sensitivity along all three directions was 150 cm/s. Total scan time for 4D-flow MRI ranged between 10 – 15 min for all patients, depending on heart rate and respiratory gating efficiency.

Data Analysis

Valve morphology and severity of aortic stenosis and insufficiency were determined using a ECG-gated segmented CINE SSFP and GRE imaging MRI sequence. ECG-gated contrast-enhanced MR angiography was used to assess aortic dimensions, which were measured both at the sinuses of Valsalva (SOV) and the mid-ascending aorta (MAA) at the level of the pulmonary artery using doubly-obliqued multiplanar reformatted images as described previously[28–30].

4D-flow MRI preprocessing—4D-flow MRI data underwent corrections for concomitant gradient fields, eddy currents, and velocity aliasing as previously described[31,32]. Noise masking and subsequent calculation of absolute blood flow velocities weighted by the magnitude data permitted the calculation of a time-averaged 3D phase contrast angiography (PC-MRA) for anatomic orientation (Figure 1) (Bock J, et al., presented at the 2007 annual meeting of the ISMRM, Abstract 3138).

4D-flow MRI analysis - semi-automated workflow—After preprocessing, 4D-flow MRI data were loaded into commercial 3D visualization software (EnSight, CEI, USA). A series of macros programmed in Python (Python Software Foundation) were developed and embedded in the visualization software for systematic step-wise 3D flow visualization and regional flow quantification.

A schematic summary of the semi-automated analysis workflow is provided in figure 2. Initially, the user adjusted the 3D-PC-MRA threshold for masking velocities inside the aorta. Next, nine analysis planes were positioned at anatomical landmarks along the thoracic aorta. The first plane was manually positioned in the aortic root, proximal to the sinuses of valsalva. The subsequent eight analysis planes were created automatically by using the location of the first plane to estimate the position and angulation of the remaining 8 planes. All plane positions were then manually shifted to defined anatomical landmarks and angulated orthogonal to the aortic lumen (plane 2 in the proximal ascending aorta (AAo), plane 3 in the AAo at the level of the right pulmonary artery, plane 4 in the AAo proximal to the origin of the brachiocephalic trunk, plane 5 between the origins of the brachiocephalic trunk and left common carotid artery, plane 6 between the origins of the left common carotid and left subclavian arteries, plane 7 in the proximal descending aorta (DAo), plane 8 in the DAo at the level of plane 1, and plane 9 in the distal DAo).

Based on the plane positioning all following steps were fully automated: Creation of time-resolved particle traces for 3D blood flow visualization in the aorta and the quantification of regional blood flow in all nine analysis planes (peak systolic velocity, net flow, regurgitation

fraction). For all 20 patients, semi-automated 4D-flow analysis was performed in a blinded fashion by two independent observers.

To evaluate the accuracy of the new semi-automated workflow, four analysis planes (aortic root, mid-ascending aorta, mid-aortic arch and proximal descending aorta) were exported from the visualization software and manually segmented for each cardiac phase by one observer using a home built tool programmed in Matlab (Matlab, The Mathworks, USA). The aortic lumen contours were manually delineated for all time-frames, and net flow, regurgitation fraction and peak systolic velocity were calculated.

Statistics

Continuous variables are reported as mean ± standard deviation. To compare hemodynamic parameters between the two patient groups (CAV cohort and tricuspid valve) a Lillifors test was used to determine parameter normalcy followed by 1-way ANOVA (normal distribution) or Kruskal Wallis (non-normal distribution). If an F or chi-squared statistic less than 0.05 determined that a hemodynamic parameter was significantly different between groups, multiple comparisons for all groups were performed. To detect statistically significant differences between groups, unpaired two-sample one-tailed t-tests were applied. For the detection of statistically significant inter-observer and inter-method differences of continuous variables, paired two-sample one-tailed t-tests were applied.

Agreement between observers and between the semi-automatic-work flow and the reference-standard (manual segmentation) was evaluated using Bland-Altman analysis[33] for flow quantification in four representative planes (aortic root, mid-AAo, mid-aortic arch and proximal DAo). From these data, mean difference ($\bar{d}$), the limits of agreement ($\bar{d} \pm 1.96$ SD) and the 95% confidence intervals ($t \cdot \sqrt{SD^2/n}$) were calculated. The appropriate *t*-value is taken from a standard *t*-distribution table in the column for $\alpha = 0.05$ and $n - 1$ degrees of freedom (with $n = 10$ and $t = 2.262$ in our study).

RESULTS

Patients' demographics are summarized in Table 1. Both patient groups were matched for all parameters except for age (the CAV group was significantly younger, $P = 0.016$) and gender (proportion of men in the CAV group = 1.2, an in the TAV group = 8). Both patient groups had aortic dilatation as expressed by SOV and MAA diameters. All patient data was successfully preprocessed and analyzed using both the semi-automated and manual analyses as illustrated for a representative patient from each cohort in Figure 2.

Analysis times for the new workflow

Processing time needed to analyze 4D-flow MRI data based on the semi-automatic workflow (plane positioning, creation of 3D particle traces, flow quantification in 9 analysis planes, see figure 2) was 40.1 ± 15.7 minutes. Manual segmentations of the vessel wall for four planes (reference method) required additional 30 minutes per patient.

Flow Quantification: Semi-automatic workflow versus manual segmentation

The results of semi-automated regional flow quantification in the aortic root, AAo, arch and DAo compared to the standard of reference method of manual lumen segmentation are summarized in Figure 3 and Table 2 (supplemental material). Good agreement was found for net flow and peak systolic velocity ($\bar{d}$<8% of mean values) compared to the reference standard while agreement was only moderate for regurgitant fraction ($\bar{d}$<41%).

Figure 4 shows an analysis plane-by-plane comparison of all flow parameters (peak velocity, net flow, regurgitation) for both CAV and TAV cohorts. Flow quantification based on the semi-automated workflow yielded similar flow parameters compared to the reference method except for regurgitant fraction in the aortic root (CAV: 2.70 ± 2.69 % vs. 2.20 ± 5.81 %, P=0.02)..

Net flow and peak velocity were similar in all analysis planes for CAV and TAV cohorts for both analysis methods. Statistically significant differences in peak systolic velocities in the DAo (CAV_{aut}: 1.03 ± 0.26 m/s, CAV_{ref}: 0.97 ± 0.22 m/s, TAV_{aut}: 0.79 ± 0.15 m/s, TAV_{ref}: 0.75 ± 0.14 m/s, P_{aut} = 0.02, P_{ref} = 0.014) were detected by both the semi-automated analysis and reference methods.

Inter-observer variability

Results of observer variability analysis for flow quantification in the aortic root, AAo, arch and DAo are summarized in Figure 5 and Table 3 (supplemental material). Bland Altman inter-observer comparisons for net flow, peak velocity, and regurgitation fraction ($\bar{d}_{netflow}$ = 8.1 ± 13.8 ml/cycle, $\bar{d}_{pvelo}$ = 0.1 ± 0.7 m/s, $\bar{d}_{regurg}$ = −0.01 ± 4.6 %) demonstrated good agreement (mean differences $\bar{d}$ < 10% of mean values) for all flow metrics.

DISCUSSION

The findings of this study systematically investigated a new standardized semi-automated analysis workflow for the evaluation of aortic hemodynamics based on 4D-flow MRI data. The application in a study cohort of 20 patients with dilation of the ascending aorta illustrated its performance compared to a reference method and its ability to detect differences in aortic flow between patients with and without trileaflet aortic valve morphology.

We found good inter-observer agreement for peak systolic velocity, net flow and regurgitant fraction, three hemodynamic parameters commonly used in the clinical routine. In addition, the comparison between the semi-automated analysis and the reference method of manual segmentation of vessel walls revealed good agreement. Variability between observers was increased at the aortic root, compared to the reference method. However, statistically significant differences in peak systolic velocity in the descending aorta between the two patient groups were detected by both methods, with an average of higher peak velocities using the semi-automated analysis method. Although the semi-automated analysis technique differed from the reference method in quantification of the retrograde fraction at the aortic root plane, the differences were small and of doubtful clinical significance.

Inter-observer and inter-method variability

For the semi-automatic analysis, calculation of flow parameters was fully automated based on aortic lumen contours as defined by the 3D PC-MRA mask. However, the PC-MR angiogram represents a time-averaged 3D mask of the thoracic aorta and may also include adjacent vessels such as the pulmonary arteries or caval veins. Incorrect plane placement or size may thus result in the inclusion of flow velocities from neighboring vessels into the flow calculations and lead to errors in flow parameters. Therefore, we investigated the variability of results compared to manually segmented vessel walls and found good accuracy for net flow and peak velocities (< 8 % variation compared with average values). However, regurgitant fraction was not as accurate with increased mean difference of approximately 40 % of the average value. We also found a significant difference in regurgitation for the two observers at the level of the aortic root. However, the average regurgitant fraction in our patient cohort was very low (4.47 % ± 7.50 %), such that the 40% mean difference corresponded to small and clinically acceptable differences of 1.8%. Future studies should therefore investigate the performance of the methods in cohorts with moderate or higher degrees of aortic valve insufficiency.

The highest variability between observers was found at the aortic root. These findings are related to the increased motion during the cardiac cycle of the aortic root compared to other aortic segments. As a result, plane placement is more challenging and the lumen contours defined by the time-averaged 3D PC-MRA mask may introduce more lumen segmentation inaccuracies. In addition, square planes used for the analysis may include flow velocities from neighboring structures such as the pulmonary artery.

However, we believe that the variability in our results is acceptable for typical clinical applications, which rely on integrated flow time curves (stroke volume, regurgitant flow) or the measurement of peak velocities (stenosis grading). Nevertheless, further investigation of the impact of these inaccuracies on flow quantification should be investigated for patient groups with severe aortic valve stenosis and/or regurgitation to evaluate the influence of more extreme flow conditions on quantification accuracy.

Sensitivity of plane placement

Regional flow quantification is sensitive to plane placement as illustrated in Figure 6 showing an example for plane placement in the mid-ascending aorta by the two observers. As evident from Figure 6, observer 2 did not fully include the entire aortic lumen in the analyses plane. In addition, different plane angulation resulted in increased partial volume error due to flow from the pulmonary artery. As a result, observer variability for all flow parameters was high for this particular patient. These findings indicate the importance of careful training of observers regarding anatomical location for plane placement and angulation.

In a previous aortic 4D-flow MRI reproducibility study by Markl et al.[27], inter-observer variability was investigated in 12 healthy volunteers. Net flow was found to be < 5 % of the total average flow and peak systolic velocity was < 3 % of the total average. In comparison, we found similar but moderately increased variability in our study cohort. However, the

previous study did only investigate aortic hemodynamics in healthy young controls and used a very time-intensive manual segmentation of aortic analysis planes. The results of our study therefore confirm the potential of a new semi-automated and more time-efficient analysis workflow for reproducible aortic 4D-flow MRI in patients with aortic dilation and congenitally altered or trileaflet aortic valve morphology.

Study limitations

Limitations of this study include the small number of patients, which underlines the feasibility nature of this study. In particular, the analysis of peak velocity and regurgitant fraction should be further analyzed in larger cohorts including sub-group analysis with more significant variance in parameters (aortic stenosis, moderate or greater aortic insufficiency, and/or aortic coarctation). Nevertheless, we were able to show that semi-automated 4D-flow analysis can provide reproducible results with good accuracy compared to manual segmentation as the standard of reference.

We investigated whether or not our new method can detect the same differences in flow parameters as found with the reference method. A drawback of this analysis is related to the analyzed parameters, which were not very sensitive to hemodynamic differences between the TAV and CAV groups. We only found differences in peak systolic velocities in the descending aorta. Future studies should thus investigate parameters such as wall shear stress that have been shown to better reflect hemodynamic differences between these cohorts[28,34].

A further limitation of this study is related to the absence of a gold standard measurement of regional aortic blood flow to evaluate the accuracy of flow parameters. The results presented in this study were based on intra-modality comparisons using semi-automated and manual aortic lumen segmentation. Future studies should additionally investigate the variability of 4D-flow MRI compared to standard 2D CINE PC MRI and flow parameters from other modalities such as Doppler echocardiography.

While the semi-automated workflow substantially reduced data analysis time (average timesaving of 7.5 minutes per analyzed segmented plane), analysis was still long (average of 40.1 minutes), which still limits the clinical application of aortic 4D-flow MRI. Further refinements and automation of the analysis workflow are thus needed to improve the interaction into a clinically feasible timeframe. For example, calculation of a centerline in the thoracic aortic lumen and automatic analysis plane placement orthogonal to the center line may help reducing the time needed for the manual refinement of plane positioning[35,36]. In addition, both analysis time and accuracy could be further increased by using a separately segmented 3D angiogram for each vascular structure of interest to improve the 3D masking of the thoracic aorta and thus avoid partial volume effects from flow velocities in adjacent vessels.

Conclusions

In conclusion, we have developed a more time-efficient semi-automated workflow for the analysis, visualization and the calculation quantitative blood flow parameters from aortic 4D-flow MRI data. Findings in two patient cohorts showed good inter-observer agreement and accuracy for net flow and peak systolic velocity. The semi-automated workflow could

detect differences in peak systolic velocities between both patient groups. Future prospective studies are needed to investigate the clinical utility of the semi-automatic 4D-flow analysis for the comprehensive evaluation of aortic valve disease.

Supplementary Material

Refer to Web version on PubMed Central for supplementary material.

ACKNOWLEDGEMENTS

Grant Support: NIH NHLBI grant R01HL115828; DFG (German Research Foundation) SCHN-1170/2-1, SIR Foundation Pilot Research Grant, and Hitachi Medical Systems/RSNA Research and Education Foundation Seed Grant RSD #1218.

LITERATURE

1. Moran PR. A flow velocity zeugmatographic interlace for NMR imaging in humans. Magn Reson Imaging. 1982; 1(4):197–203. [PubMed: 6927206]
2. Firmin DN, Nayler GL, Kilner PJ, et al. The application of phase shifts in NMR for flow measurement. Magn Reson Med. 1990; 14(2):230–241. [PubMed: 2345505]
3. Wigstrom L, Sjoqvist L, Wranne B. Temporally resolved 3D phase-contrast imaging. Magn Reson Med. 1996; 36(5):800–803. [PubMed: 8916033]
4. Markl M, Chan FP, Alley MT, et al. Time-resolved three-dimensional phase-contrast MRI. J Magn Reson Imaging. 2003; 17(4):499–506. [PubMed: 12655592]
5. Frydrychowicz A, Harloff A, Jung B, et al. Time-resolved, 3-dimensional magnetic resonance flow analysis at 3 T: visualization of normal and pathological aortic vascular hemodynamics. J Comput Assist Tomogr. 2007; 31(1):9–15. [PubMed: 17259827]
6. Hope TA, Markl M, Wigstrom L, et al. Comparison of flow patterns in ascending aortic aneurysms and volunteers using four-dimensional magnetic resonance velocity mapping. J Magn Reson Imaging. 2007; 26(6):1471–1479. [PubMed: 17968892]
7. Bammer R, Hope TA, Aksoy M, et al. Time-resolved 3D quantitative flow MRI of the major intracranial vessels: initial experience and comparative evaluation at 1.5T and 3.0T in combination with parallel imaging. Magn Reson Med. 2007; 57(1):127–140. [PubMed: 17195166]
8. Varaprasathan GA, Araoz PA, Higgins CB, et al. Quantification of flow dynamics in congenital heart disease: applications of velocity-encoded cine MR imaging. Radiographics. 2002; 22(4):895–905. discussion 905–6. [PubMed: 12110719]
9. Markl M, Harloff A, Bley TA, et al. Time-resolved 3D MR velocity mapping at 3T: improved navigator-gated assessment of vascular anatomy and blood flow. J Magn Reson Imaging. 2007; 25(4):824–831. [PubMed: 17345635]
10. Hope TA, Herfkens RJ. Imaging of the thoracic aorta with time-resolved three-dimensional phase-contrast MRI: a review. Semin Thorac Cardiovasc Surg. 2008; 20(4):358–364. [PubMed: 19251177]
11. Hope MD, Sedlic T, Dyverfeldt P. Cardiothoracic magnetic resonance flow imaging. J Thorac Imaging. 2013; 28(4):217–230. [PubMed: 23708687]
12. Markl M, Frydrychowicz A, Kozerke S, et al. 4D flow MRI. J Magn Reson Imaging. 2012; 36(5): 1015–1036. [PubMed: 23090914]
13. Wentland AL, Grist TM, Wieben O. Repeatability and internal consistency of abdominal 2D and 4D phase contrast MR flow measurements. Acad Radiol. 2013; 20(6):699–704. [PubMed: 23510798]
14. Clough R, Taylor P. Future imaging techniques in aortic pathologies and clinical implications. J Cardiovasc Surg (Torino). 2013; 54 Suppl 1(1):15–19.

15. Nordmeyer S, Riesenkampff E, Messroghli D, et al. Four-dimensional velocity-encoded magnetic resonance imaging improves blood flow quantification in patients with complex accelerated flow. J Magn Reson Imaging. 2013; 37(1):208–216. [PubMed: 22976284]
16. Valverde I, Simpson J, Schaeffter T, et al. 4D phase-contrast flow cardiovascular magnetic resonance: comprehensive quantification and visualization of flow dynamics in atrial septal defect and partial anomalous pulmonary venous return. Pediatr Cardiol. 2010; 31(8):1244–1248. [PubMed: 20848278]
17. Bogren HG, Buonocore MH, Valente RJ. Four-dimensional magnetic resonance velocity mapping of blood flow patterns in the aorta in patients with atherosclerotic coronary artery disease compared to age-matched normal subjects. J Magn Reson Imaging. 2004; 19(4):417–427. [PubMed: 15065165]
18. Buonocore MH. Visualizing blood flow patterns using streamlines, arrows, and particle paths. Magn Reson Med. 1998; 40(2):210–226. [PubMed: 9702703]
19. Kozerke S, Hasenkam JM, Pedersen EM, et al. Visualization of flow patterns distal to aortic valve prostheses in humans using a fast approach for cine 3D velocity mapping. J Magn Reson Imaging. 2001; 13(5):690–698. [PubMed: 11329190]
20. Eriksson J, Carlhall CJ, Dyverfeldt P, et al. Semi-automatic quantification of 4D left ventricular blood flow. J Cardiovasc Magn Reson. 2010; 12:9. [PubMed: 20152026]
21. Frayne R, Steinman DA, Ethier CR, et al. Accuracy of MR phase contrast velocity measurements for unsteady flow. J Magn Reson Imaging. 1995; 5(4):428–431. [PubMed: 7549205]
22. Ley S, Unterhinninghofen R, Ley-Zaporozhan J, et al. Validation of magnetic resonance phase-contrast flow measurements in the main pulmonary artery and aorta using perivascular ultrasound in a large animal model. Invest Radiol. 2008; 43(6):421–426. [PubMed: 18496047]
23. Harloff A, Zech T, Wegent F, et al. Comparison of Blood Flow Velocity Quantification by 4D Flow MR Imaging with Ultrasound at the Carotid Bifurcation. AJNR Am J Neuroradiol. 2013; 34(7):1407–1413. [PubMed: 23413247]
24. Goo HW, Al-Otay A, Grosse-Wortmann L, et al. Phase-contrast magnetic resonance quantification of normal pulmonary venous return. J Magn Reson Imaging. 2009; 29(3):588–594. [PubMed: 19243041]
25. Powell AJ, Maier SE, Chung T, et al. Phase-velocity cine magnetic resonance imaging measurement of pulsatile blood flow in children and young adults: in vitro and in vivo validation. Pediatr Cardiol. 2000; 21(2):104–110. [PubMed: 10754076]
26. Westenberg JJ, Danilouchkine MG, Doornbos J, et al. Accurate and reproducible mitral valvular blood flow measurement with three-directional velocity-encoded magnetic resonance imaging. J Cardiovasc Magn Reson. 2004; 6(4):767–776. [PubMed: 15646879]
27. Markl M, Wallis W, Harloff A. Reproducibility of flow and wall shear stress analysis using flow-sensitive four-dimensional MRI. J Magn Reson Imaging. 2011; 33(4):988–994. [PubMed: 21448968]
28. Barker AJ, Markl M, Burk J, et al. Bicuspid aortic valve is associated with altered wall shear stress in the ascending aorta. Circ Cardiovasc Imaging. 2012; 5(4):457–466. [PubMed: 22730420]
29. Hiratzka LF, Bakris GL, Beckman JA, et al. 2010 ACCF/AHA/AATS/ACR/ASA/SCA/SCAI/SIR/STS/SVM Guidelines for the diagnosis and management of patients with thoracic aortic disease. A Report of the American College of Cardiology Foundation/American Heart Association Task Force on Practice Guidelines, American Association for Thoracic Surgery, American College of Radiology, American Stroke Association, Society of Cardiovascular Anesthesiologists, Society for Cardiovascular Angiography and Interventions, Society of Interventional Radiology, Society of Thoracic Surgeons,and Society for Vascular Medicine. J Am Coll Cardiol. 2010; 55(14):e27–e129. [PubMed: 20359588]
30. Bonow RO, Carabello BA, Chatterjee K, et al. 2008 focused update incorporated into the ACC/AHA 2006 guidelines for the management of patients with valvular heart disease: a report of the American College of Cardiology/American Heart Association Task Force on Practice Guidelines (Writing Committee to revise the 1998 guidelines for the management of patients with valvular heart disease). Endorsed by the Society of Cardiovascular Anesthesiologists, Society for Cardiovascular Angiography and Interventions, and Society of Thoracic Surgeons. J Am Coll Cardiol. 2008; 52(13):e1–e142. [PubMed: 18848134]

31. Walker PG, Cranney GB, Scheidegger MB, et al. Semiautomated method for noise reduction and background phase error correction in MR phase velocity data. J Magn Reson Imaging. 1993; 3(3): 521–530. [PubMed: 8324312]

32. Bernstein MA, Zhou XJ, Polzin JA, et al. Concomitant gradient terms in phase contrast MR: analysis and correction. Magn Reson Med. 1998; 39(2):300–308. [PubMed: 9469714]

33. Bland JM, Altman DG. Statistical methods for assessing agreement between two methods of clinical measurement. Lancet. 1986; 1(8476):307–310. [PubMed: 2868172]

34. Hope MD, Hope TA, Crook SE, et al. 4D flow CMR in assessment of valve-related ascending aortic disease. JACC Cardiovasc Imaging. 2011; 4(7):781–787. [PubMed: 21757170]

35. Spottiswoode, B.; Stalder, A.; Gulsun, M., et al. Proc Intl Soc Mag Reson Med 2013, 21: 1342. Salt Lake City, USA: 2013. Semi-automated pulse wave velocity measurement in the thoracic aorta using 4D flow MRI. Abstract: 1342

36. Stalder, AF.; Gulsun, MA.; Greiser, A., et al. Proc Intl Soc Mag Reson Med 2013, 21: 1434. Salt Lake City, USA: 2013. Fully automatic visualization of 4D Flow data. Abstract: 1434

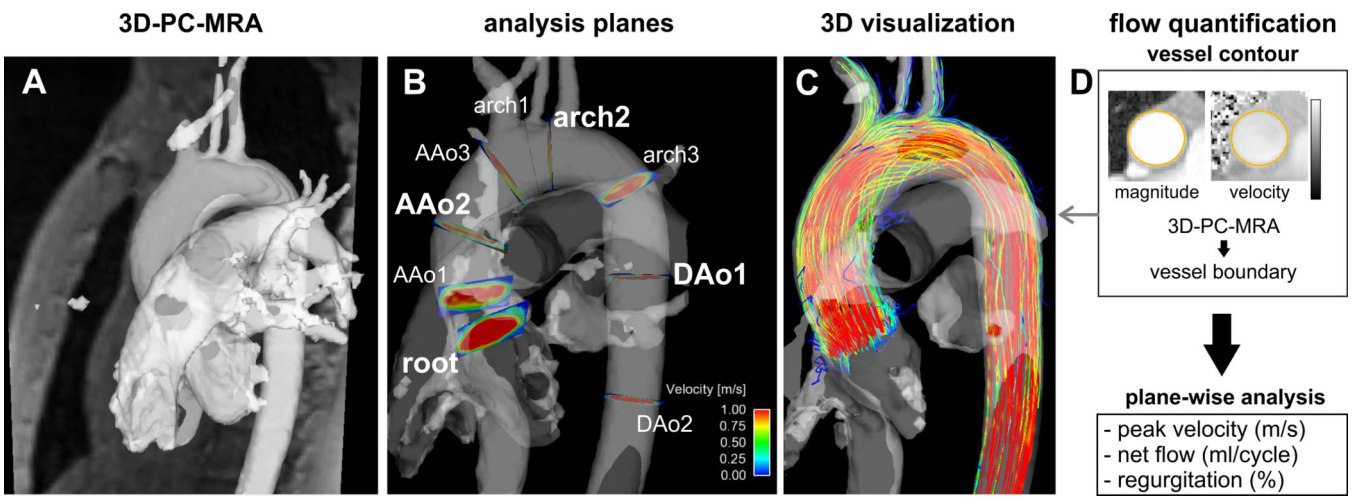

Fig. 1.

Summary of the workflow from left to right: A. PC-MRA and the magnitude image loaded into the visualization software. B. Positioning of 9 analysis planes along the aorta. The four planes used for further quantification are highlighted in bold type. C. Calculation of time-resolved particle traces with the PC-MRA as a mask. D. Flow quantification of peak velocity, net flow and regurgitation using the 3D-PC-MRA as a mask for the vessel boundaries for each analysis plane.

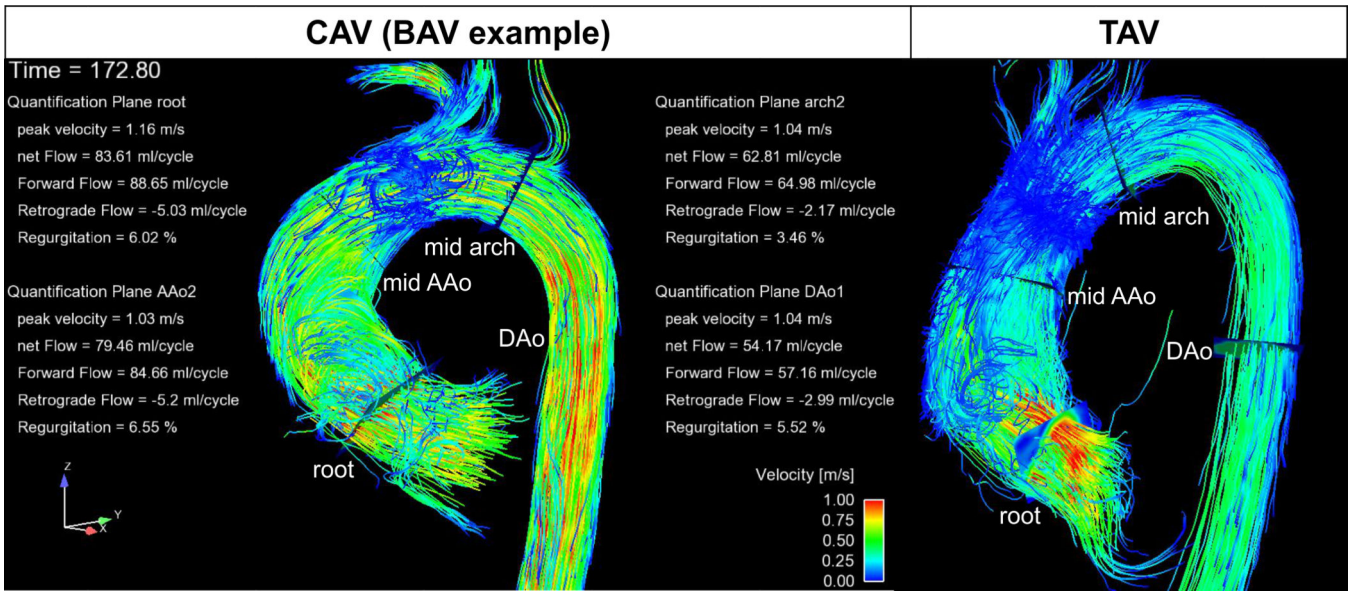

Fig. 2.

Examples of semi-automated 3D flow visualization and flow quantification for a CAV and a TAV patient. 3D blood flow is visualized using systolic 3D streamlines.

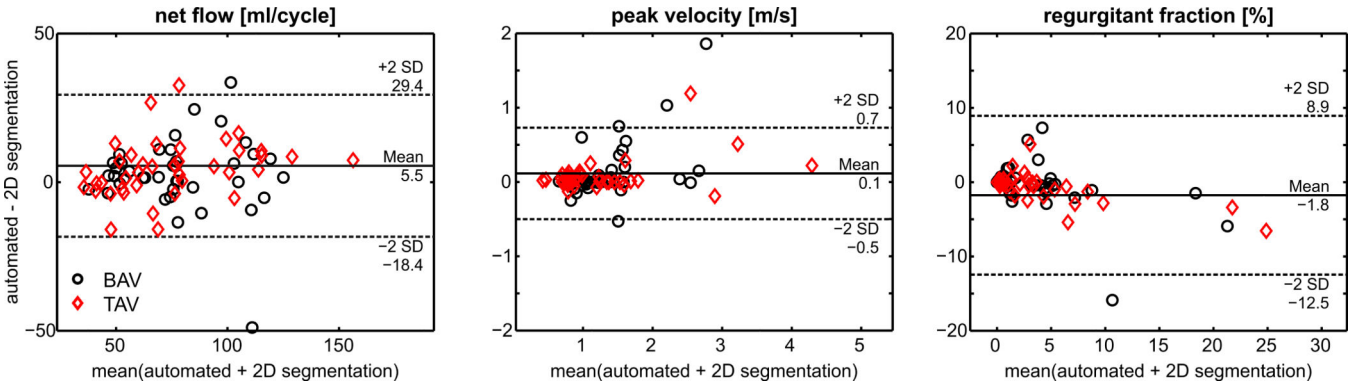

Fig. 3.

Bland-Altman analysis of flow quantification based on the semi-automatic workflow compared to the reference method (manual segmentation of the vessel wall) for net flow, peak velocity and regurgitant fraction.

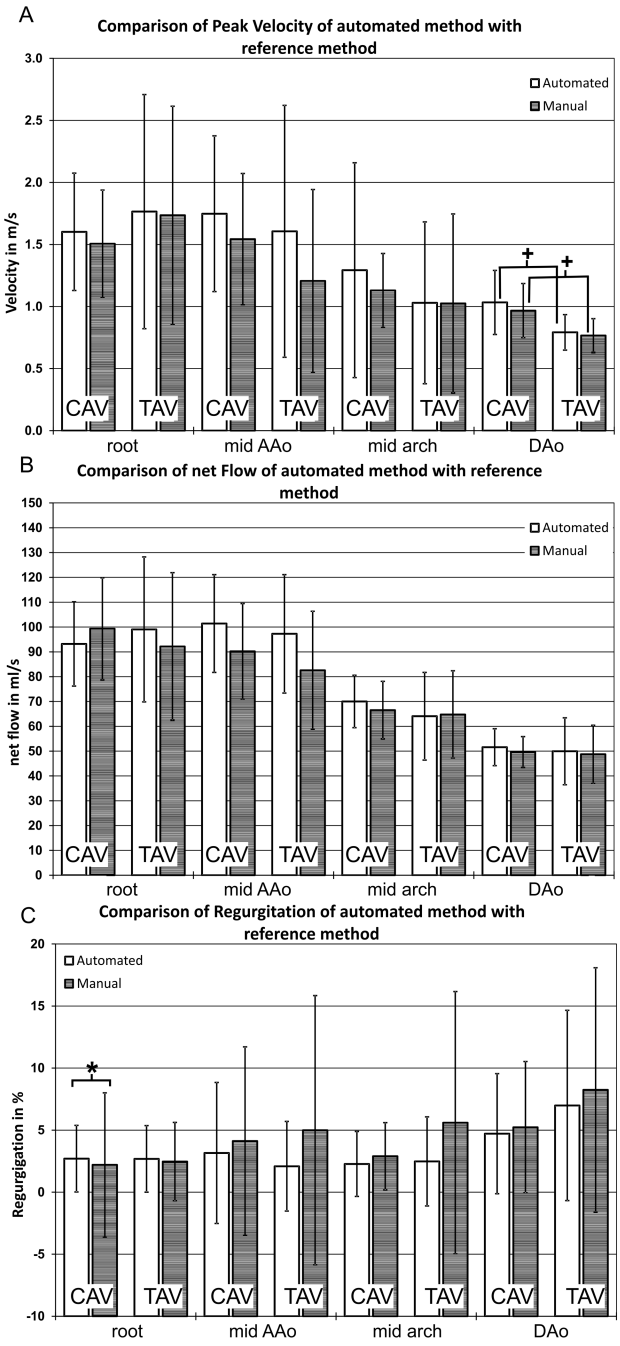

Fig. 4.

Comparison of flow quantification based on the semi-automated workflow (white column) with the reference method (manual segmentation) for both patient groups and all analysis planes. A: peak systolic velocities B: net flow C: regurgitant fraction. * indicates significant differences between the new method and the reference method ($p < 0.05$, paired two-sampled paired t-test). + indicates significant differences between the two patient groups ($p < 0.05$, unpaired two-sampled t-test).

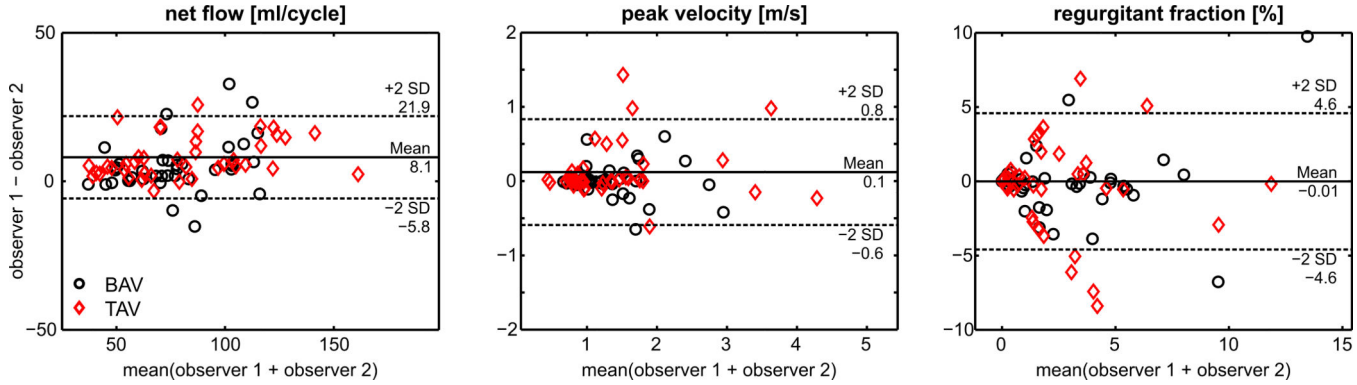

Fig. 5.

Bland-Altman plots for inter observer variability for net flow, peak velocity and regurgitant fraction.

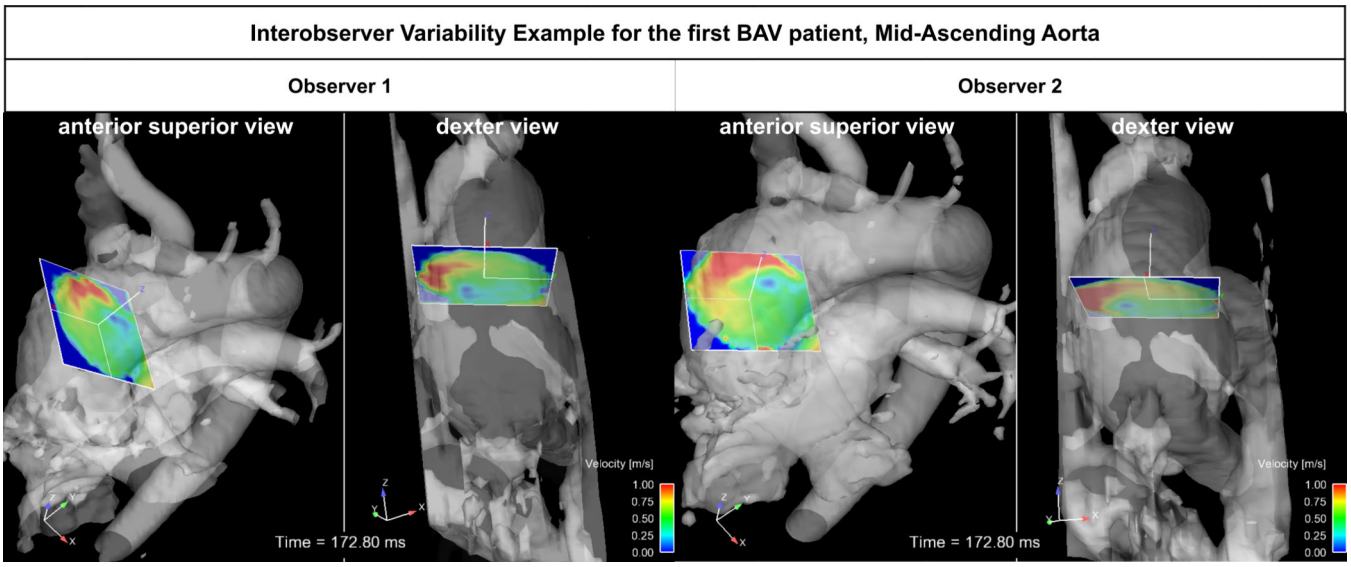

Fig. 6.

Inter-observer variability of analysis plane placement in a CAV patient analyzed by two observers. For each observer, an anterior superior view and on the right the dexter view is shown.

Table 1

Patients' demographics (CAV = bicuspid aortic valve, TAV = tricuspid aortic valve, Ao = aorta, SOV = sinuses of valsalva, MAA = mid-ascending aorta)

Parameter	CAV	TAV
Age	46.7 ± 8.9*	55.5 ± 5.9*
Gender	6M, 5F	8M, 1F
Height in cm	180.1 ± 11.7	176.7 ±6.2
Weight in kg	81.0 ± 14.4	91.5 ± 20.8
Stroke Volume in ml	82.2 ± 16.8	89.2 ± 31.1
SOV diameter in cm	4.2 ± 0.6	4.3 ± 0.5
MAA diameter in cm	3.9 ± 1.1	4.3 ± 0.4
Ao Stenosis	1 severe, 1 mild to moderate	2 moderate
Ao Insufficiency	1 severe, 2 mild, 1 trace	3 mild, 1 trace
Aneurysm	9	all
Valve	10 Bicuspid, 1 Quadricuspid	9 Tricuspid
Valve Fusion pattern	5 R/N, 5 R/L	-

* indicates significant difference ($p<0.05$) using an unpaired t-test (for normal distributed data) or the Mann-Whitney U-test (for not normal distributed data).